

Evaluating the vegetation growing season changes in the arid region of northwestern China

Yanfang Wang · Yanjun Shen · Fubao Sun · Yanning Chen

Received: 20 March 2013 / Accepted: 18 December 2013
© Springer-Verlag Wien 2014

Abstract Temperature has long been accepted as the major controlling factor in determining vegetation phenology in the middle and higher latitudes. The influence of water availability is often overlooked even in arid and semi-arid environments. We compared vegetation phenology metrics derived from both in situ temperature and satellite-based normalized difference vegetation index (NDVI) observations from 1982 to 2006 by an example of the arid region of northwestern China. From the satellite-based results, it was found the start of the growing season (SOS) advanced by 0.37 days year⁻¹ and the end of the growing season (EOS) delayed by 0.61 days year⁻¹ in Southern Xinjiang over 25 years. In the Tianshan Mountains, the SOS advanced by 0.35 days year⁻¹ and the EOS delayed by 0.31 days year⁻¹. There were almost no changes in Northern Xinjiang. Compared with satellite-based results, those estimates based on temperature contain less details of spatial variability of vegetation phenology. Interestingly, they show

different and at times reversed spatial patterns from the satellite results arising from water limitation. Phenology metrics derived from temperature and NDVI conclude that water limitation of onset of the growing season is more severe than the cessation. Phenology spatial patterns of four oases in Southern Xinjiang show that, on average, there is a delay of the SOS of 1.6 days/10 km of distance from the mountain outlet stations. Our results underline the importance of water availability in determining the vegetation phenology in arid regions and can lead to important consequences in interpreting the possible change of vegetation phenology with climate.

1 Introduction

Vegetation phenology, the annual rhythm of biological phenomena, has received increasing attention over the last several decades particularly in temperate regions (White et al. 1997; Piao et al. 2006; Peñuelas et al. 2009; Gordo and Sanz 2010; Korner and Basler 2010). It rises because many organisms alter their life cycles in response to ongoing climate change. At the same time, phenology feedbacks are important to the hydrological and climatic systems by influencing the seasonality of albedo, surface roughness length, and fluxes of water, energy, and CO₂ (Richardson et al. 2013). For example, recent studies have shown that, across temperate regions, temperature is the most important controlling factor (Piao et al. 2006; Primack and Miller-Rushing 2011). As most of those studies were concentrated in temperate regions, temperature-based phenology models are widely accepted using the strong linkage between seasonal temperature variability and phenological changes (Chmielewski 2003; Fisher et al. 2007; Jiang et al. 2011; Shen et al. 2012). Phenology, however, has been studied less in extreme climate environments despite being more vulnerable to climate change (Primack and Miller-Rushing 2011).

Y. Wang · Y. Shen
Key Laboratory of Agricultural Water Resources, Hebei Key Laboratory of Agricultural Water-Saving, Center for Agricultural Resources Research, Institute of Genetics and Developmental Biology, Chinese Academy of Sciences, Shijiazhuang 050021, China

Y. Wang
University of Chinese Academy of Sciences, Beijing 10049, China

Y. Wang · F. Sun
Research School of Biology, The Australian National University, Canberra 0200, Australia

Y. Chen
Xinjiang Institute of Ecology and Geography, The Chinese Academy of Sciences, Urumqi 830011, China

Y. Shen (✉)
Center for Agricultural Resources Research, Institute of Genetics and Developmental Biology, Chinese Academy of Sciences, Shijiazhuang 050021, China
e-mail: yjshen@sjziam.ac.cn

In theory, in arid regions, the ecosystem and hydrological cycles are expected to be sensitive to water availability (Budyko 1974). Here, arid regions are defined by the aridity index, the ratio between mean annual precipitation and potential evapotranspiration (<0.2), and cover 20 % of global land area (Shen and Chen 2010). Sparse vegetation in arid regions is a key terrestrial biome and exerts a strong control on the water cycle in dryland areas (Maestre et al. 2012; Wang et al. 2012). Vegetation in arid regions is highly vulnerable to desertification and highly sensitive to global climate change (Eswaran et al. 1999; Lioubimtseva 2004; Salguero-Gomez et al. 2012). As global warming continues to progress, it is important to detect vegetation signals comprehensively and correctly such as vegetation coverage, biomass, and phenology in these areas.

In recent years, satellite-derived information is being demonstrated as an important method in detecting regional phenological variability (White et al. 1997; Piao et al. 2006; Busetto et al. 2010; Davison et al. 2011; Jeong et al. 2011; Shen et al. 2012), due to its advantage of being able to produce long-term, large-scale, and continuous observations. The normalized difference vegetation index (NDVI), taking advantage of the drastic difference between red and near-infrared light reflected by a healthy plant, is widely used as a proxy indicator of vegetation productivity (Gomez-Mendoza et al. 2008; Fensholt et al. 2012). Remotely sensed vegetation phenology involves non-traditional metrics (e.g., germination, flowering, leaf expansion, color changing, leaf fall, etc.), which is capable of capturing key information regarding the onset, cessation, and length of growing season by greenness. All of this phenological information assists in gaining insight into ecosystem susceptibility to natural and anthropogenic perturbations, which is important in arid regions, where ecosystems are highly vulnerable to disturbance (Kong et al. 2010).

Xinjiang province in the northwest of China contains the second largest shifting sand desert in the world, the Taklamakan Desert, as well as the longest inland river in China, the Tarim River. In line with unprecedented global warming being experienced since the 1980s (Corfee-Morlot et al. 2007), increasing trends of mean annual temperature, precipitation, and river runoff were observed in Xinjiang around the same time (Shi et al. 2007). Hence, investigation of vegetation phenological changes occurring with climate change and anthropogenic activities from this period is critical to establish a framework for sustainable management of ecosystems in this arid region. Research tries to draw the phenology of this area from a temperate-system concept (Jiang et al. 2011). However, phenology in arid regions is more complex than that in most temperate systems because water availability, as a principal trigger of phenology, is highly variable and relatively unpredictable (Peñuelas et al. 2004; Primack and Miller-Rushing 2011; Buyantuyev and Wu 2012; Richardson et al. 2013).

The primary objective of this study is to detect spatial patterns and trends in vegetation phenology in arid regions

by taking Xinjiang Province in Northwestern China from 1982 to 2006 as a case study. Specifically, this study aims to (1) examine the differences between phenology metrics from the traditional thermal method based on surface meteorological measurements of temperatures and those from the remotely sensed vegetation index-based methods, (2) examine how water limitation influences spatial patterns of phenology in arid areas, and (3) examine trends in vegetation phenology in different areas of the study region across the period 1982–2006. The research extends the phenology study to previously overlooked extreme climate environments—arid regions. We analyzed regional phenology with not only the response to temperature and precipitation but also the response to river discharge, which is important to determinate the phenology of oasis vegetation (Buyantuyev and Wu 2012).

2 Materials and methods

2.1 Study area

The study area of Xinjiang province, located in northwestern China, extends longitudinally from 73°24' E to 97°00' E and latitudinally from 34°50' N to 49°15' N, with a total area of 1.66×10^6 km² (Fig. 1a). It is the largest arid region in China, and precipitation is <100 mm year⁻¹ in most areas owing to the dominance of the continental arid climate and less effects of the East Asian Monsoon (Shen et al. 2010). Highly influenced by elevation (from -154 to 7,400 m), there is a strong spatial heterogeneity in the hydro-climatic conditions, which form different ecoregions, e.g. the Mountain Ecoregion, Diluvial fan Ecoregion, and Desert Ecoregion. The landscape characteristics include desert matrix, vegetation patch, and river corridor (Fig. 1b). Irrigated cropland in the diluvial fan oasis covers only 5 % of the land surface, but supports 95 % of the population (about 21.8 million in Xinjiang in 2010) in the area (Wen and Jin 2012). In this study, the region was divided into three zones, including Northern Xinjiang, the Tianshan Mountains, and Southern Xinjiang, according to geographical location and climatic characteristics. Mean annual temperature and precipitation (1982–2006) from meteorological stations show different climatic characteristics among these areas (Table 1). The Tianshan Mountains area is relatively wet but with the lowest temperature, as opposed to, Southern Xinjiang which has the highest temperature but the lowest precipitation. Northern Xinjiang is in between.

2.2 Methods

2.2.1 Phenology metrics from traditional thermal method

In traditional phenological studies of temperate zones, air temperature is regarded as the main trigger of vegetation

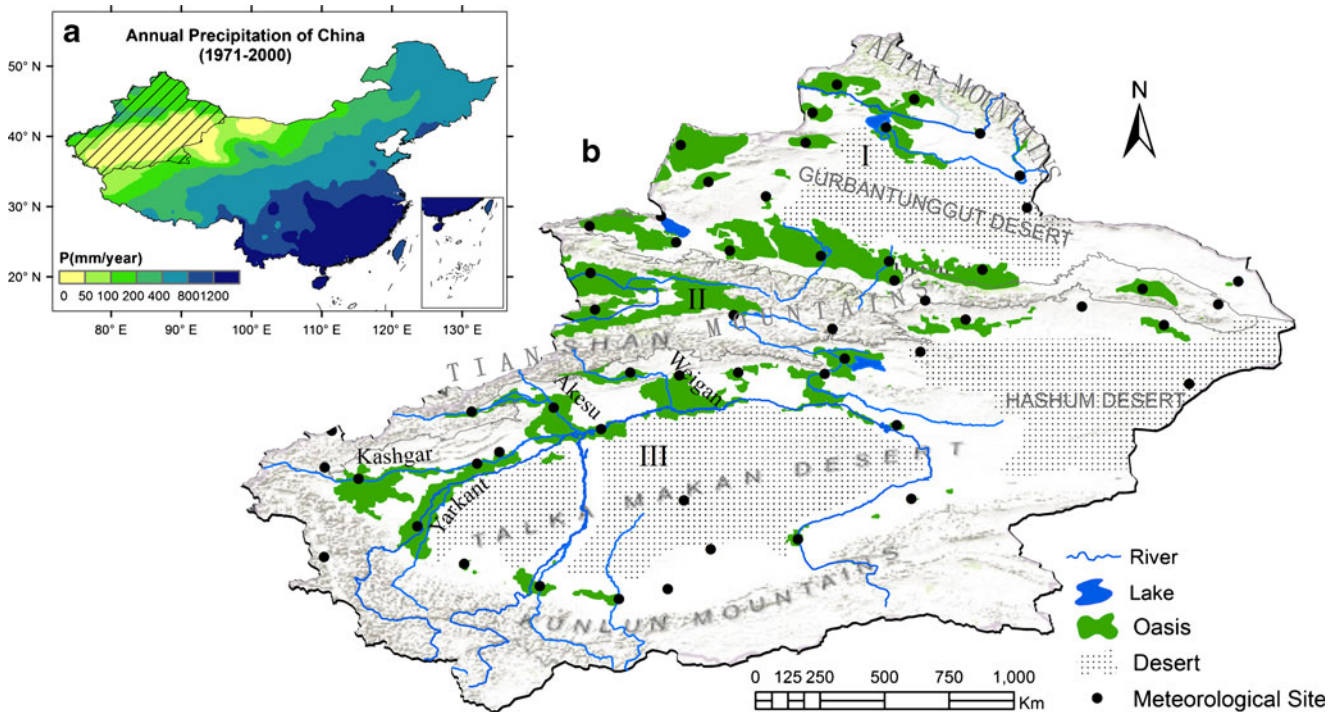


Fig. 1 Study area. **a** Location of the study area of Xinjiang province with background of mean annual precipitation of China from 1971 to 2000. **b** Distribution of rivers, oases, and meteorological observation

sites with rendering topography background (WGS-84 reference frame) and three partitions of the region: *I* Northern Xinjiang, *II* Tianshan Mountains, and *III* Southern Xinjiang

phenology, as extended, for example, to northwestern China (Jiang et al. 2011). The start of the growing season (SOS) is defined as the first appearance of five consecutive days with daily average temperatures (T) higher than $5\text{ }^{\circ}\text{C}$. Similarly, the end of the growing season (EOS) is defined as the last appearance of five consecutive days with $T > 5\text{ }^{\circ}\text{C}$ in autumn. We adopt this definition and used daily temperature data of 53 in situ meteorological observation sites in Xinjiang from the China Meteorological Administration.

2.2.2 Phenology metrics from vegetation index

National Oceanic and Atmospheric Administration–Advanced Very High Resolution Radiometer (AVHRR) NDVI, which is capable of providing long-term statistics (1982–2006), has been extensively used to detect and monitor vegetation dynamics related to climate variability and land-use changes at both regional and global levels (Ji et al. 2008; Fensholt et al. 2012).

Table 1 Mean annual temperature (MAT) and precipitation (MAP) and their standard deviation (STD) derived from 53 meteorological stations (1982–2006)

	MAT ($^{\circ}\text{C}$)	STD ($^{\circ}\text{C}$)	MAP (mm)	STD (mm)
Northern Xinjiang	6.1	2.4	167.3	55.2
Tianshan Mountains	4.0	4.8	252.5	108.6
Southern Xinjiang	11.1	2.2	62.7	27.6

We used a calibrated version on the basis of those data, i.e., AVHRR Global Inventory Modeling and Mapping Studies (GIMMS) NDVI, which has reduced influences from view geometry, volcanic aerosols, and others not related to actual vegetation change (Tucker et al. 2005). The data are at 15-day intervals with a spatial resolution of 8 km.

Satellite derived phenology is generally based on the idea that canopy greenness observed from satellites is related to canopy development (Fisher et al. 2007). Some key phenology information, such as the SOS, and the EOS can be derived from the satellite-measured NDVI data. Generally, data filter and interpolation are needed to smooth out the noise around NDVI time series and disaggregate to daily data before being used. Then, different threshold methods can be used to detect phenology metrics; these include the absolute threshold, the dynamic ratio threshold, and abrupt change method (Table 2).

To minimize bias, we applied these three methods (Fig. 2). Firstly, the Savitzky–Golay filter was applied to eliminate the noise in the original NDVI series. Then, the three methods above were used to derive SOS and EOS from polynomial fitting lines of the first and the last half year. In the absolute threshold method, we choose 0.15 as the threshold to identify the growth of vegetation of this region, and ratios of 0.2 and 0.5 are respectively for SOS and EOS in the dynamic ratio threshold, slightly revised for EOS from Yu et al. (2010) for this specific study area. The abrupt change method from Piao et al. (2006) is also used (Piao et al. 2006; Jeong et al. 2011).

Table 2 Summarized methods used to derive phenology metrics from satellite-based NDVI data (the methods in the bold font are used in the paper)

Data filter and interpolation	The Best Index Slope Extraction (White et al. 1997) Fourier analysis (Jia et al. 2011) The Savitzky–Golay filter (Brown et al. 2010) Wavelet-based filter (Sakamoto et al. 2010) Asymmetric Gaussian function fitting (Jonsson and Eklundh 2002) Logistic function fitting (Zhang et al. 2004; Busetto et al. 2010; Li et al. 2010) Polynomial fitting method (Piao et al. 2006; Jeong et al. 2011)
Threshold determination	Absolute threshold , e.g. 0.17 (Fischer 1994), 0.09 (Jia et al. 2004), etc. Dynamic ratio threshold , e.g. 20 or 50 % of the annual maximum amplitude (difference between annual maximum and minimum NDVI) (White et al. 1997; Jonsson and Eklundh 2004; Brown et al. 2010; Yu et al. 2010) Abrupt change (also called sudden change in some previous studies) in NDVI, which is by identifying the time period when there is an “abrupt increase or abrupt decrease” in the NDVI (Zhang et al. 2004; Piao et al. 2006).

Three methods were used to derive the phenology threshold from the 25-year average vegetation growing curve for each pixel to derive the average phenology pattern of years. Then, the calculated NDVI threshold of each pixel was used to determine the onset dates of vegetation green-up and dormancy for each year.

3 Results

3.1 Spatial pattern of phenology

3.1.1 Temperature-based phenology pattern

The temperature-based phenology pattern varies depending on geographical position and elevation (Figs. 3a and 4a). It is

the same as we expected according to mean annual temperature in Table 1. The earliest SOS, occurring in March, mainly appears in the oases of Southern Xinjiang. Later, in April, SOS occurs in the oases of Northern Xinjiang and a few oases at the higher latitude of Southern Xinjiang. The latest occur at the high altitude of Tianshan Mountains with SOS of later than 120 days of year (DOY; according to the Julian calendar). The spatial results of the EOS are generally opposite to the SOS as indicated in Fig. 4a. The temperature-based EOS is delayed from the Tianshan Mountains to Northern Xinjiang, and Southern Xinjiang.

3.1.2 Satellite-based phenology pattern

Using the satellite-based NDVI data, we can observe a more detailed pattern of phenology (Fig. 3b–d) than that from air temperature. The earliest SOS appearing in early March is mainly distributed in the Gurbantunggut desert of Northern Xinjiang and some oases in the Tianshan Mountains and Northern Xinjiang. Northern Xinjiang region, especially, in the Gurbantunggut desert, contains many early spring desert ephemeral plants, which are capable of taking advantage of rainfall in early spring and complete their life cycles in a short time (Zhang et al. 2011). Note that the results of absolute method in the Gurbantunggut desert are later than the others because the threshold of 0.15 is somehow too high for desert ephemeral plants. Later, the SOS in late March–early April is mainly in the upstream of oases in Southern Xinjiang and most parts of Northern Xinjiang. The upstream of Southern Xinjiang oases has a higher temperature owing to the lower latitude, and water is supplied by the early spring flood produced by the snow melt in the mountains. However, the SOS in the middle and lower reaches of oases is delayed due to the time lags of water availability.

The earliest EOS from NDVI is mainly distributed in the mountain areas of the three regions, which is the same as the temperature-based results. Later EOS appears in most of the oasis areas both in Southern and Northern Xinjiang. Ephemeral plants in the Gurbantunggut desert and parts of the oases in Tianshan Mountains and Northern Xinjiang are the latest.

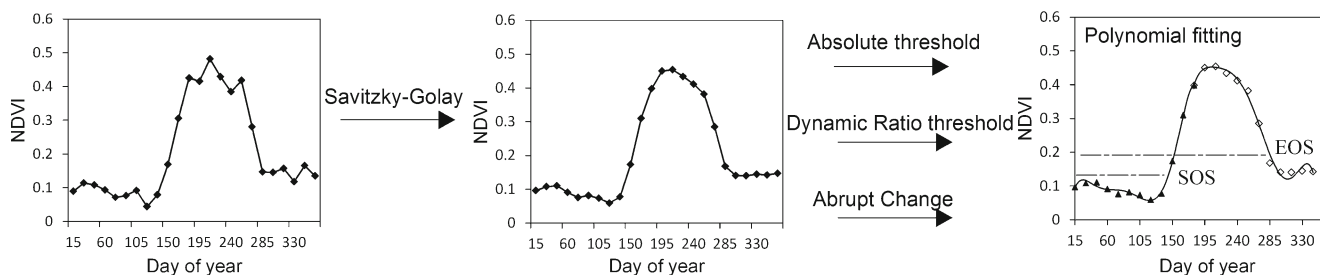
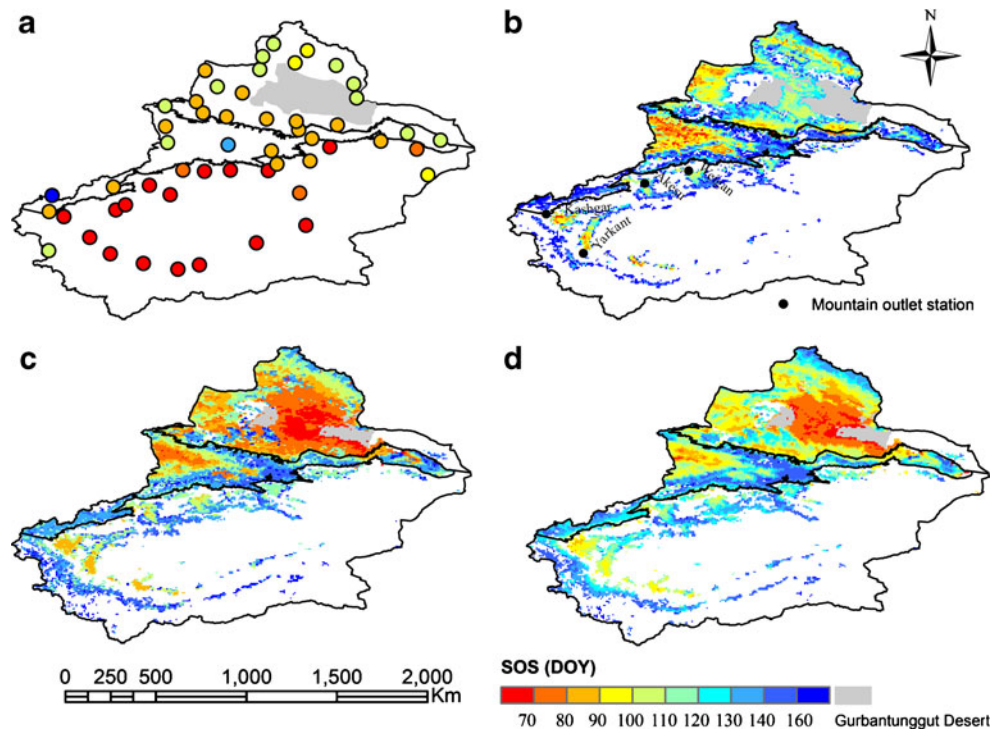
**Fig. 2** Flow chart of getting phenology metrics from original NDVI series (SOS/EOS start/end of the growing season). The filled triangles and hollow diamonds are the first and the last half year

Fig. 3 Mean annual phenology pattern of start of the growing season (SOS) based on **a** temperature, **b** vegetation index absolute threshold, **c** vegetation index dynamic ratio threshold, and **d** vegetation index abrupt change method



3.1.3 Comparison of phenology patterns between the temperature-based and satellite-based results

Generally, differences between temperature-based and satellite-based EOS results (mean value of 5 days) are much less than those of SOS (mean value of 31 days) as shown in Table 3. It

indicates that water limitation on the SOS is more severe than that on the EOS. In terms of the spatial pattern, in Northern Xinjiang, the annual mean temperature is relatively low (Table 1), but the growing season begins earliest observed from NDVI. After that is the Tianshan Mountains area. In Southern Xinjiang, we estimated the earliest SOS from the temperature-

Fig. 4 Mean annual phenology pattern of end of the growing season based on **a** temperature, **b** vegetation index absolute threshold, **c** vegetation index dynamic ratio threshold, and **d** vegetation index abrupt change method

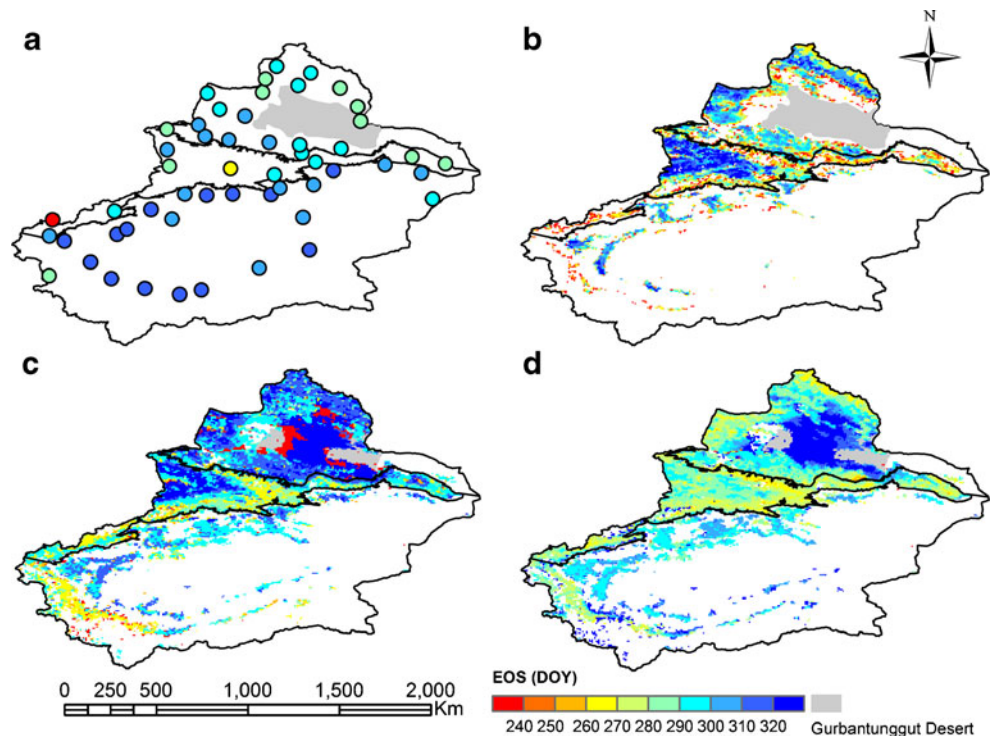


Table 3 Statistics of vegetation phenology for three regions

	SOS					EOS				
	AT	DRT	AC	T	STD	AT	DRT	AC	T	STD
Southern Xinjiang	147	128	132	73	32	281	300	292	309	12
Tianshan Mountains	130	123	122	106	10	286	284	296	285	6
Northern Xinjiang	120	98	94	94	12	284	300	303	295	8

SOSEOS start/end of the growing season, *AT* vegetation index Absolute threshold, *DRT* vegetation index Dynamic Ratio threshold, *AC* vegetation index Abrupt Change method, *T* temperature method, *STD* standard deviation

based method, but observed the latest SOS from the satellite-based NDVI data. Water limitation has played a vital role in generating the generally inverse patterns among the three regions. Similar situation happened in the EOS. However, for each region, standard deviation of the EOS of the four methods is much smaller than that of the SOS (Table 3).

3.1.4 Comparison of spring phenology between the upstream and downstream

Examination of the phenology spatial pattern within the four oases in Southern Xinjiang indicates that the SOS is delayed along rivers (Fig. 3b–d) although the air temperature is almost identical (Fig. 3a). Detailed information about the four river basins and the corresponding oases is shown in Table 4. For each oasis, it shows a delayed pattern with increasing distance between location in the oases and its corresponding mountain outlet station (Figs. 3b and 5). The differences of phenology arise because the oasis vegetation is generally controlled by the available water from rivers. The closer is the distance to the mountain outlet means the earlier is the water arrival. With the increasing distance, an oscillation exists owing to different threshold methods with the natural vegetation around the oases. It shows that the time series of the absolute threshold method have the largest variability, and the ones of dynamic

ratio threshold are the most stable. Within each oasis, the results show slightly different delayed speeds of SOS, which are 1.7, 1.9, 1.1, and 1.6 days/10 km (significance level $p < 0.05$) for the Yarkant Oasis, the Kashgar Oasis, the Akesu Oasis, and the Weigan Oasis in Southern Xinjiang, respectively. On average, SOS is delayed by 1.6 days of per 10 km distance from the runoff stations. However, the phenology estimated based on surface temperature cannot capture the above detailed information.

3.2 Phenology trends

3.2.1 Temperature-based phenology trend

Phenology trends were derived by nonparametric Mann–Kendall Trend test method from both temperature- and satellite-based phenology results from 1982 to 2006. According to the statistical value of 1.96 at significance level of 0.05, trends are divided into significant advanced trend (SAT), significant delayed trend (SDT), and nonsignificant trend (NT). The result from temperature indicates the significant advanced SOS trend mainly appears in Southern Xinjiang and several stations in the Tianshan Mountains (Fig. 6a). Most parts of Northern Xinjiang, the Tianshan Mountains, and east part of Southern Xinjiang are mainly nonsignificant. The significant delayed EOS also is mainly distributed in the north of the Kunlun Mountains in Southern Xinjiang from temperature results (Fig. 8a). Stations in the Tianshan Mountains and Northern Xinjiang are nonsignificant. It indicates that the significant prolonged thermal growing season mainly appears in Southern Xinjiang, especially in the north of Kunlun Mountains.

3.2.2 Satellite-based phenology trend

However, the satellite-based SOS is not exactly the same as that from temperature (Fig. 6b–d). The significant advanced SOS is mainly distributed in the oases of south of Southern Xinjiang and scatters in Northern Xinjiang and the Tianshan Mountains. The SOS trend in most parts of Northern Xinjiang

Table 4 Summarized information about four river basins and their oases in Southern Xinjiang, including the length of the rivers, relief in elevation, and 1982–2006 mean annual runoff (MAR) of the river basins; the

25-year mean annual temperature (MAT), mean annual precipitation (MAP), oasis relief in elevation, and the start of the growing season (SOS) delayed speed with the distance to mountain outlet station

	River Basin			Oasis				
	Length (km)	Relief (m)	MAR (10^8 m^3)	MAT ($^{\circ}\text{C}$)	MAP (mm)	Relief (m)	Length (km)	SOS delayed (days/10 km)
Yarkant	970	400–7,244	67.6	12.0	73.4	1,077–1,768	400	1.7
Kashgar	900	1126–7,351	38.6	12.2	61.0	1,139–1,562	300	1.9
Akesu	530	984–6,172	67.7	10.7	65.1	997–1,079	180	1.1
Weigan	452	921–6,553	27.9	11.2	77.4	928–1,114	220	1.6

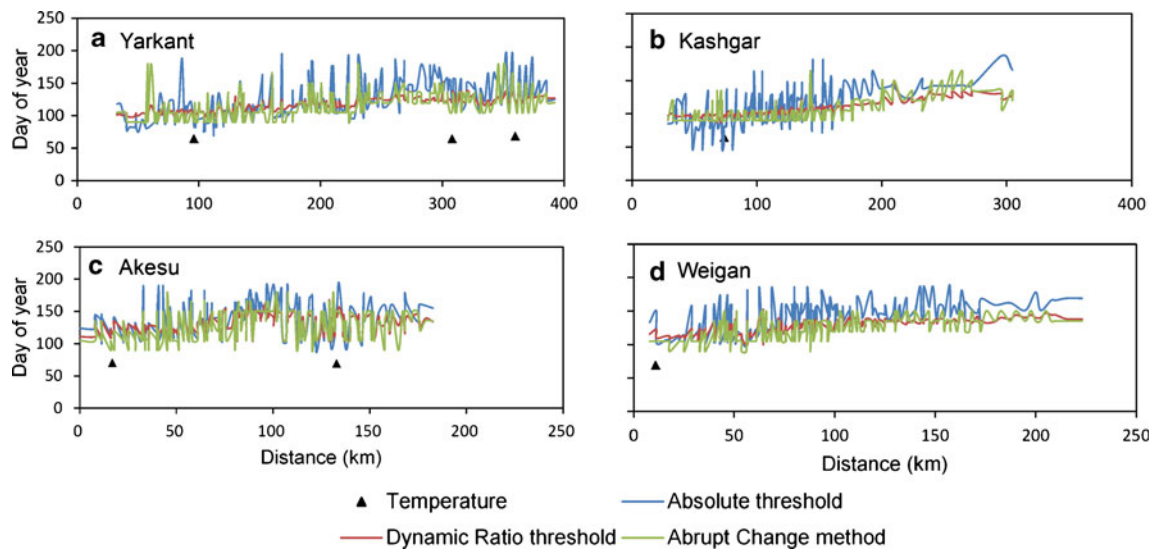


Fig. 5 Variations of the start of the growing season with increasing distance between oasis position and its corresponding mountain outlet station in Southern Xinjiang (location of oases **a–d** and corresponding mountain runoff hydrological stations are indicated in Fig. 3b)

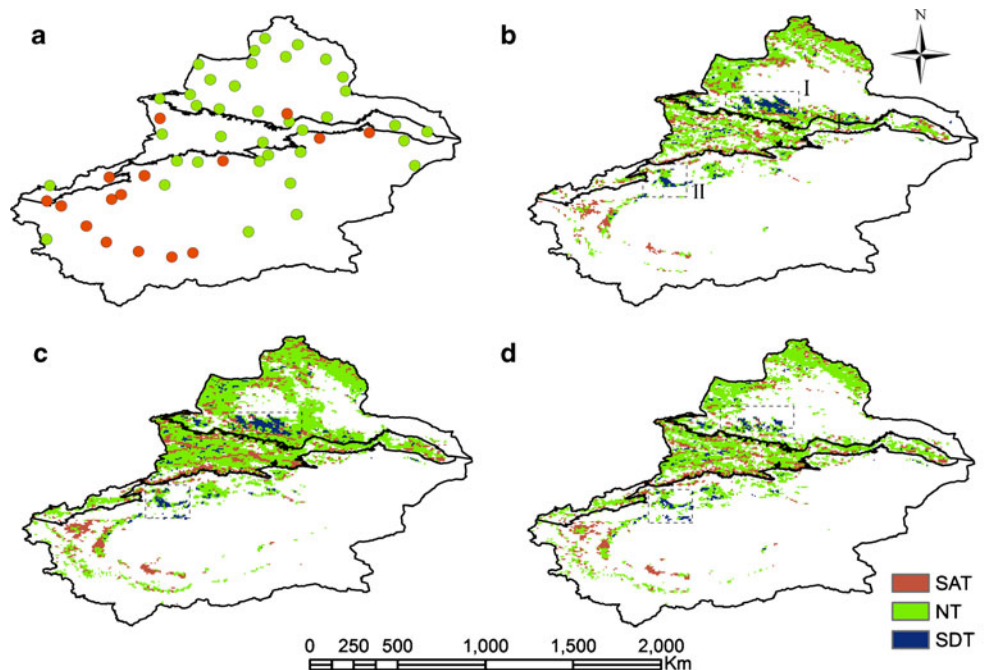
and Tianshan Mountains is nonsignificant. But other than that, there are two oasis parts showing significant delayed SOS in Northern Xinjiang and Southern Xinjiang (Fig. 6b). Five-year-average NDVI growing curves of the two delayed parts are shown in Fig. 7. It obviously shows a decreased NDVI in spring and an increased NDVI in summer, which results in a delayed SOS. We checked the change of agriculture structure of these two places and found that they were both the areas of changing from wheat and corn to cotton (Kang and Zhu 2008; Shen, et al. 2013). The NDVI derived EOS shows a significant delayed trend in Southern Xinjiang and the Altai Mountains, and most of the other parts are nonsignificant (Fig. 8b–d).

Only some desert and cultivated vegetation shows significant advanced trend.

3.2.3 Comparison of trends for different regions

Overall, the 25-year phenological time series of the three regions derived from NDVI are shown in Fig. 9. Linear regression results indicate that the advanced SOS and delayed EOS trends are mainly significant in the Tianshan Mountains and Southern Xinjiang (at significance level p of 0.05). In Southern Xinjiang, the delayed EOS ($0.61 \text{ days year}^{-1}$, $p=0.02$) is much longer than the advanced SOS ($0.37 \text{ days year}^{-1}$, $p=0.03$)

Fig. 6 Trends of the start of the growing season from methods of **a** temperature, **b** vegetation index absolute threshold, **c** vegetation index dynamic ratio threshold, and **d** vegetation index abrupt change method. *SAT* significant advanced trend, *NT* nonsignificant trend, *SDT* significant delayed trend (oases in the north of Tianshan Mountains (*I*) and the Akesu oasis (*II*) with significant delayed trends are analyzed below in detail)



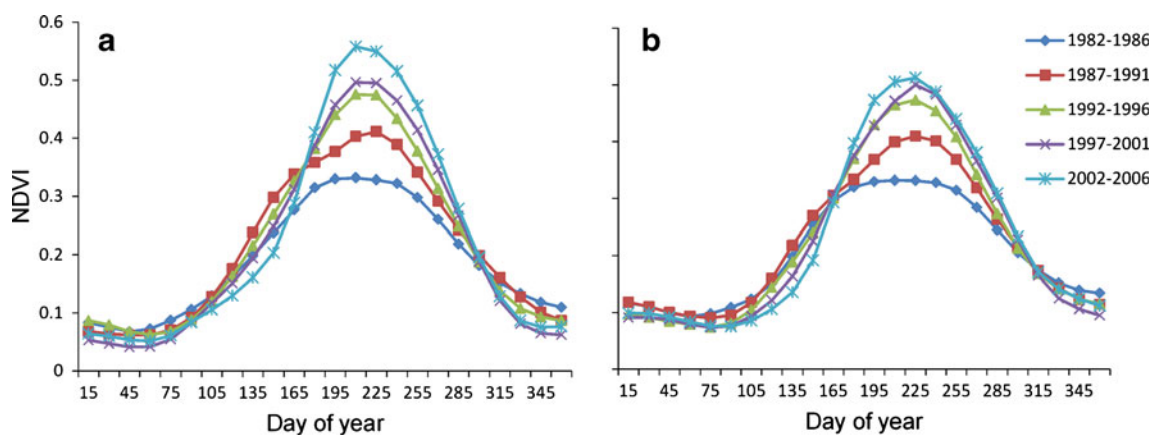


Fig. 7 The 5-year average vegetation growing curve of significant delayed the start of the growing season (SOS) in *I* **a** Northern Xinjiang and *II* **b** Southern Xinjiang (*I* and *II* indicated in Fig. 6b)

(Fig. 9a, b). The timing of phenology events changed more quickly in autumn compared with the spring. Both advanced SOS and delayed EOS are similar in Tianshan Mountains, $0.35 \text{ days year}^{-1}$ ($p=0.007$) and $0.31 \text{ days year}^{-1}$ ($p=0.06$), respectively (Fig. 9c, d). The result in Northern Xinjiang is unique from the others. The SOS and EOS changed ambiguously, and no obvious trend was shown (Fig. 9e, f).

4 Discussion

4.1 Ephemeral plants in the Gurbantunggut Desert

The spatial pattern of phenology shows that both the earliest SOS and latest EOS appear in the Gurbantunggut Desert (see gray areas in both Figs. 3 and 4), and there is an absence of

values in the results of the absolute threshold method from the satellite-based NDVI data. Here, we prepared a plot to show the annual NDVI growing curve averaged across the Gurbantunggut Desert (Fig. 10), which was not well represented by the absolute threshold method. It contains two peaks on the 145 and 273 days of year, and the two corresponding NDVI values are 0.13 and 0.12, respectively, which are lower than the threshold of 0.15 being chosen.

In the Gurbantunggut Desert, ephemeral plants are the main vegetation types and play a key role in desert ecosystem stability and environmental conservation including *Tamarix ramosissima*, *Haloxylon ammodendro*, *Haloxylon persicum*, *Ephedra distachya*, *Ephedra oxorrhynchum*, etc. (Mao and Zhang 1994; Zhang et al. 2011). Of them, desert ephemeral plants are mainly distributed throughout Central Asia, the Mediterranean seashore, West Asia, and North Africa, etc.

Fig. 8 Trends of the end of the growing season from methods of **a** temperature, **b** vegetation index absolute threshold, **c** vegetation index dynamic ratio threshold, **d** vegetation index abrupt change method (*SAT* significant advanced trend, *NT* nonsignificant trend, *SDT* significant delayed trend)

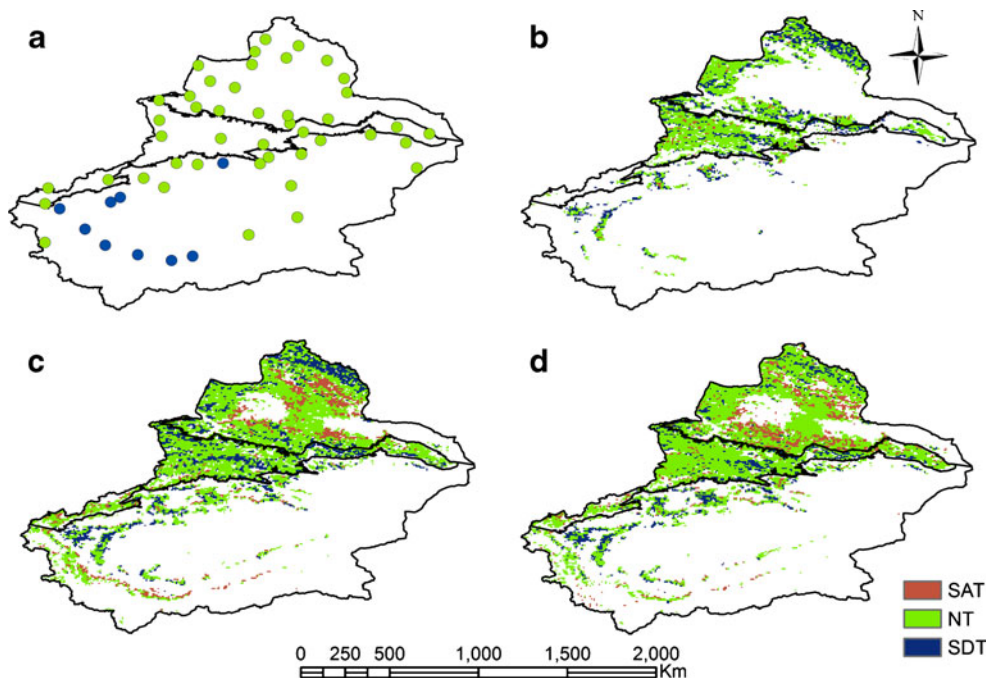
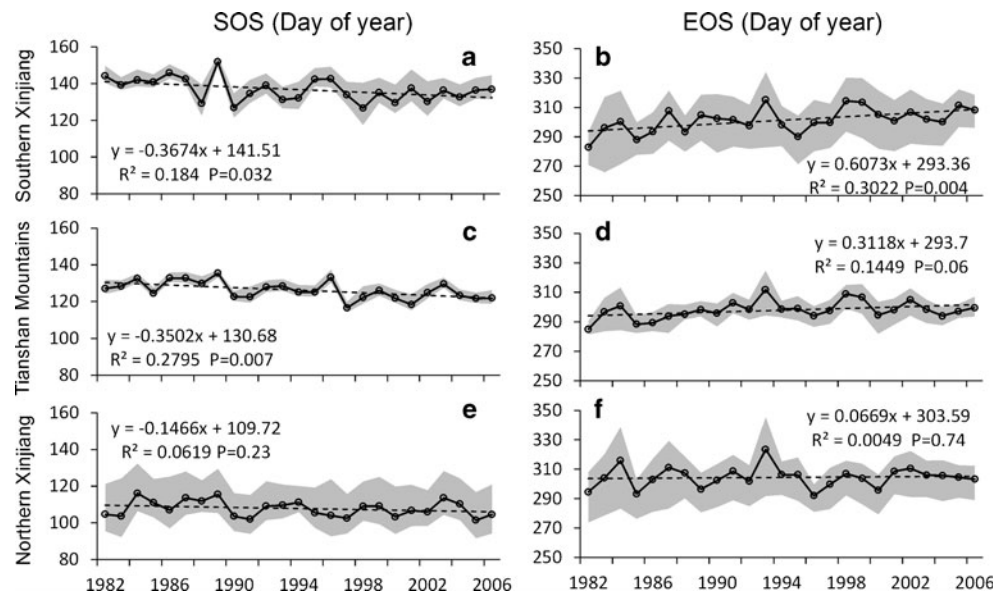


Fig. 9 The averaged satellite based phenology trends including start of the growing season (*SOS*) and end of the growing season (*EOS*) of three regions from 1982 to 2006 (gray areas are the range of estimates by the three methods)



(Li 2010). As the 15-day-interval NDVI growing curve averaged across the Gurbantunggut Desert (Fig. 10), vegetation growth resumes a few days after the first rain or melting-snow water in early spring with the average SOS being the 73rd day of the Julian calendar. The results reported here that the maximal NDVI value appears in early May and most ephemeral annual plants complete growth and reproduction in about 2 or 3 months are consistent with field observations (Zhang et al. 2012b). Detailed field observations also show that, after ephemeral life circle in early summer, some ephemerals germinate during summer (Wang et al. 2006) and another NDVI peak appears in September. However, the peak in September is lower as the number of species and plant height are both significantly lower than those in spring (see Fig. 10).

4.2 Ecological and agricultural implications of phenology shifts under climate warming in arid regions

A longer presence of the green cover in large areas may alter land surface physical processes by influencing the seasonality of albedo, surface roughness, canopy conductance, latent and

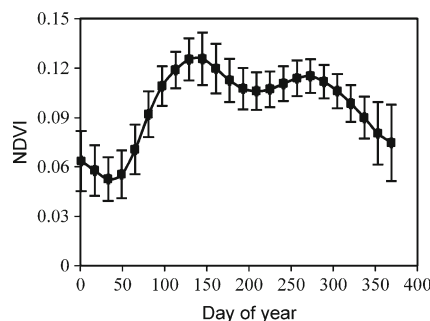


Fig. 10 Annual NDVI growing curve averaged across the Gurbantunggut Desert 1982–2006 with \pm standard deviation

sensible heat, turbulence, terrestrial carbon (C) sink, and biogenic volatile organic compounds (Peñuelas et al. 2009; Xia and Wan 2012; Richardson et al. 2013). All these changes can have tremendous effects on the geo-ecological environment in arid regions where ecology is vulnerable. The beginning of the growing season is strongly controlled by the date of snow and ice melting in this region. Therefore, earlier warmer temperatures will lead to not only thermal but also water availability by earlier snow melt. The glaciers have shrunk due to temperature increase since the 1950s, and this retreat has accelerated over the past 20 years (Zhang et al. 2012a). It is not sustainable for the regional ecology, although the warming has increased the vegetation coverage in the short term. Meanwhile, the prolonged growing season means that even more water is required than previously, and may result in soil moisture depletion, which could put negative effects on ecosystems in a long run.

Timing of phenological events and their variability have had measurable impacts on the development and production of field crops, including the changes in the farming system and crop yield (Tao et al. 2006; Sacks and Kucharik 2011). In accordance with the warmer climate, earlier onset of spring and longer growing season prevail, which may lead finally to higher and more stable crop yields and improved food quality. However, the effects of prolonged growing season are contradictory. The longer growing season also will increase pest's reproductive cycles and consume more irrigated water. The earlier onset of greenness holds, at the same time, the danger of damages by late frosts (Chmielewski 2003).

5 Conclusions

1. In this study, we show that the satellite-based observation can reflect the spatial patterns of vegetation phenology

with more detail than those based on temperature. The difference between them is suggested to be due to various water limitations in arid regions. Based on the same NDVI data, we estimated the phenology using three commonly used methods, and they keep pace with the overall spatial pattern and temporal trend while with some discrepancies.

2. According to the first part of the results, water limitation of SOS is more severe than EOS across the whole study area. Of them, water limitation in Southern Xinjiang is more severe than that in Northern Xinjiang. Examination of the spatial pattern of phenology within four oases in Southern Xinjiang indicates that, on average, over the 25 years, the SOS is dependent on the distance from the mountain outlet station. On average, this impact is estimated as a delayed SOS at 1.6 days/10 km within those oases with the increasing distance to mountain outlet station.
3. Average trends of the three methods show a more significant phenology change in the southern part than the northern regions. A significant advance of the SOS of 0.37 days year⁻¹ ($p=0.03$) and delay of the EOS of 0.61 days year⁻¹ ($p=0.02$) are shown in Southern Xinjiang during 1982 to 2006. Both the advance of the SOS and the delay of the EOS are similar in the Tianshan Mountains, 0.35 days year⁻¹ ($p=0.007$) and 0.31 days year⁻¹ ($p=0.06$), respectively. The results in Northern Xinjiang are ambiguous, and no obvious trend is shown.
4. Satellite-based phenology also can reflect the variations that influenced by anthropogenic activities through changing farming systems. However, the traditional thermal method derived from temperature cannot capture the actual change in vegetation phenology in arid regions. Of particular importance here, at a regional scale such as the study area, possible changes in water availability and temperature are generally different or even on the opposite direction. The difference of phenology pattern between the temperature-based estimate method and satellite-based vegetation measurement reported here can lead to important consequences in interpreting the possible influence of climate change on vegetation phenology change in arid regions.

Acknowledgments This study was supported by the National Program on Key Basic Research Project of China (2010CB951003). The author, Yanfang Wang, thanks the financial support from the China Scholarship Council (CSC). GIMMS NDVI dataset and vegetation type data were provided by Environmental and Ecological Science Data Center for West China, National Natural Science Foundation of China (<http://westdc.westgis.ac.cn>). The authors would like to thank the reviewers for their helpful remarks.

References

- Brown ME, de Beurs K, Vrieling A (2010) The response of African land surface phenology to large scale climate oscillations. *Remote Sens Environ* 114(10):2286–2296. doi:10.1016/j.rse.2010.05.005
- Budyko MI (1974) *Climate and life*. Academic, New York
- Busetto L, Colombo R, Migliavacca M, Cremonese E, Meroni M, Galvagno M, Rossini M, Siniscalco C, Di Cella UM, Pari E (2010) Remote sensing of larch phenological cycle and analysis of relationships with climate in the Alpine region. *Glob Chang Biol* 16(9):2504–2517. doi:10.1111/j.1365-2486.2010.02189.x
- Buyantuyev A, Wu J (2012) Urbanization diversifies land surface phenology in arid environments: interactions among vegetation, climatic variation, and land use pattern in the Phoenix metropolitan region, USA. *Landscape and Urban Planning* 105(1):149–159. doi:10.1016/j.landurbplan.2011.12.013
- Chmielewski F-M (2003) Phenology and agriculture. In: Schwartz M (ed) *Phenology: an integrative environmental science*. Springer, Berlin, pp 505–522
- Corfee-Morlot J, Maslin M, Burgess J (2007) Global warming in the public sphere. *Philosophical Transactions of the Royal Society a-Mathematical Physical and Engineering Sciences* 365(1860):2741–2776. doi:10.1098/rsta.2007.2084
- Davison JE, Breshears DD, van Leeuwen WJD, Casady GM (2011) Remotely sensed vegetation phenology and productivity along a climatic gradient: on the value of incorporating the dimension of woody plant cover. *Glob Ecol Biogeogr* 20(1):101–113. doi:10.1111/j.1466-8238.2010.00571.x
- Eswaran H, Reich P, Beinroth F (1999) Global desertification tension zones. In: *Sustaining the global farm. Selected papers from the 10th international soil conservation organization meeting*, vol 29, pp 24–28
- Fensholt R, Langanke T, Rasmussen K, Reenberg A, Prince SD, Tucker C, Scholes RJ, Le QB, Bondeau A, Eastman R, Epstein H, Gaughan AE, Hellden U, Mbow C, Olsson L, Paruelo J, Schweitzer C, Seaquist J, Wessels K (2012) Greenness in semi-arid areas across the globe 1981–2007—an earth observing satellite based analysis of trends and drivers. *Remote Sens Environ* 121:144–158. doi:10.1016/j.rse.2012.01.017
- Fischer A (1994) A model for the seasonal-variations of vegetation indexes in coarse resolution data and its inversion to extract crop parameters. *Remote Sens Environ* 48(2):220–230. doi:10.1016/0034-4257(94)90143-0
- Fisher JL, Richardson AD, Mustard JF (2007) Phenology model from surface meteorology does not capture satellite-based greenup estimations. *Glob Chang Biol* 13(3):707–721. doi:10.1111/j.1365-2486.2006.01311.x
- Gomez-Mendoza L, Galicia L, Cuevas-Fernandez ML, Magana V, Gomez G, Palacio-Prieto JL (2008) Assessing onset and length of greening period in six vegetation types in Oaxaca, Mexico, using NDVI-precipitation relationships. *Int J Biometeorol* 52(6):511–520. doi:10.1007/s00484-008-0147-6
- Gordo O, Sanz JJ (2010) Impact of climate change on plant phenology in Mediterranean ecosystems. *Glob Chang Biol* 16(3):1082–1106. doi:10.1111/j.1365-2486.2009.02084.x
- Jeong S-J, Ho C-H, Gim H-J, Brown ME (2011) Phenology shifts at start vs. end of growing season in temperate vegetation over the Northern Hemisphere for the period 1982–2008. *Glob Chang Biol* 17(7):2385–2399. doi:10.1111/j.1365-2486.2011.02397.x
- Ji L, Gallo K, Eidenshink JC, Dwyer J (2008) Agreement evaluation of AVHRR and MODIS 16-day composite NDVI data sets. *International Journal of Remote Sensing* 29(16):4839–4861. doi:10.1080/01431160801927194
- Jia GJ, Epstein HE, Walker DA (2004) Controls over intra-seasonal dynamics of AVHRR NDVI for the Arctic tundra in northern Alaska. *International Journal of Remote Sensing* 25(9):1547–1564. doi:10.1080/0143116021000023925
- Jia L, Shang H, Hu G, Menenti M (2011) Phenological response of vegetation to upstream river flow in the Heihe River basin by time series analysis of MODIS data. *Hydrology and Earth System Sciences* 15(3):1047–1064. doi:10.5194/hess-15-1047-2011
- Jiang FQ, Hu RJ, Zhang YW, Li XM, Tong L (2011) Variations and trends of onset, cessation and length of climatic growing season over

- Xinjiang, NW China. *Theor Appl Climatol* 106(3–4):449–458. doi:10.1007/s00704-011-0445-5
- Jonsson P, Eklundh L (2002) Seasonality extraction by function fitting to time-series of satellite sensor data. *Geoscience and Remote Sensing, IEEE Transactions on* 40(8):1824–1832. doi:10.1109/TGRS.2002.802519
- Jonsson P, Eklundh L (2004) TIMESAT—a program for analyzing time-series of satellite sensor data. *Comput Geosci* 30(8):833–845. doi:10.1016/j.cageo.2004.05.006
- Kang J, Zhu M (2008) The historical and substantial evidence analysis of Xinjiang agricultural production structure. *The border economy and culture* 6:3–5 (In Chinese)
- Kong WJ, Sun OJX, Chen YN, Yu Y, Tian ZQ (2010) Patch-level based vegetation change and environmental drivers in Tarim River drainage area of West China. *Landsc Ecol* 25(9):1447–1455. doi:10.1007/s10980-010-9505-y
- Korner C, Basler D (2010) Phenology under global warming. *Science* 327(5972):1461–1462. doi:10.1126/science.1186473
- Li X (2010) Biology of annual plants in arid and semi-arid desert regions of China. In: Weidinger T (ed) *Desert plants*. Springer, Berlin, pp 73–89
- Li M, Qu JJ, Hao XJ (2010) Investigating phenological changes using MODIS vegetation indices in deciduous broadleaf forest over continental U.S. during 2000–2008. *Ecological Informatics* 5(5):410–417. doi:10.1016/j.ecoinf.2010.04.002
- Lioubimtseva E (2004) Climate change in arid environments: revisiting the past to understand the future. *Progress in Physical Geography* 28(4):502–530. doi:10.1191/0309133304pp422oa
- Maestre FT, Salguero-Gómez R, Quero JL (2012) It is getting hotter in here: determining and projecting the impacts of global environmental change on drylands. *Philosophical Transactions of the Royal Society B: Biological Sciences* 367(1606):3062–3075. doi:10.1098/rstb.2011.0323
- Mao Z, Zhang D (1994) Conspectus of ephemeral flora in northern Xinjiang. *Arid Zone Research* 11(3):1–26
- Peñuelas J, Filella I, Zhang X, Llorens L, Ogaya R, Lloret F, Comas P, Estiarte M, Terradas J (2004) Complex spatiotemporal phenological shifts as a response to rainfall changes. *New Phytologist* 161(3):837–846. doi:10.1111/j.1469-8137.2004.01003.x
- Peñuelas J, Rutishauser T, Filella I (2009) Phenology feedbacks on climate change. *Science* 324(5929):887–888. doi:10.1126/science.1173004
- Piao SL, Fang JY, Zhou LM, Ciais P, Zhu B (2006) Variations in satellite-derived phenology in China's temperate vegetation. *Glob Chang Biol* 12(4):672–685. doi:10.1111/j.1365-2486.2006.01123.x
- Primack RB, Miller-Rushing AJ (2011) Broadening the study of phenology and climate change. *New Phytologist* 191(2):307–309. doi:10.1111/j.1469-8137.2011.03773.x
- Richardson AD, Keenan TF, Migliavacca M, Ryu Y, Sonnentag O, Toomey M (2013) Climate change, phenology, and phenological control of vegetation feedbacks to the climate system. *Agr Forest Meteorol* 169:156–173. doi:10.1016/j.agrformet.2012.09.012
- Sacks WJ, Kucharik CJ (2011) Crop management and phenology trends in the US Corn Belt: Impacts on yields, evapotranspiration and energy balance. *Agr Forest Meteorol* 151(7):882–894. doi:10.1016/j.agrformet.2011.02.010
- Sakamoto T, Wardlow BD, Gitelson AA, Verma SB, Suyker AE, Arkebauer TJ (2010) A two-step filtering approach for detecting maize and soybean phenology with time-series MODIS data. *Remote Sens Environ* 114(10):2146–2159. doi:10.1016/j.rse.2010.04.019
- Salguero-Gomez R, Siewert W, Casper BB, Tielborger K (2012) A demographic approach to study effects of climate change in desert plants. *Philosophical Transactions of the Royal Society B-Biological Sciences* 367(1606):3100–3114. doi:10.1098/rstb.2012.0074
- Shen YJ, Chen YN (2010) Global perspective on hydrology, water balance, and water resources management in arid basins. *Hydrological Processes* 24(2):129–135. doi:10.1002/hyp.7428
- Shen YJ, Liu CM, Liu M, Zeng Y, Tian CY (2010) Change in pan evaporation over the past 50 years in the arid region of China. *Hydrological Processes* 24(2):225–231. doi:10.1002/Hyp.7435
- Shen MG, Tang YH, Chen J, Yang W (2012) Specification of thermal growing season in temperate China from 1960 to 2009. *Clim Change* 114(3–4):783–798. doi:10.1007/s10584-012-0434-4
- Shen YJ, Li S, Chen YN, Qi YQ, Zhang SW (2013) Estimation of regional irrigation water requirement and water supply risk in the arid region of Northwestern China 1989–2010. *Agricultural Water Management* 128:55–64. doi:10.1016/j.agwat.2013.06.014
- Shi YF, Shen YP, Kang E, Li DL, Ding YJ, Zhang GW, Hu RJ (2007) Recent and future climate change in northwest china. *Clim Change* 80(3–4):379–393. doi:10.1007/s10584-006-9121-7
- Tao F, Yokozawa M, Xu Y, Hayashi Y, Zhang Z (2006) Climate changes and trends in phenology and yields of field crops in China, 1981–2000. *Agr Forest Meteorol* 138(1):82–92. doi:10.1016/j.agrformet.2006.03.014
- Tucker CJ, Pinzon JE, Brown ME, Slayback DA, Pak EW, Mahoney R, Vermote EF, El Saleou N (2005) An extended AVHRR 8-km NDVI dataset compatible with MODIS and SPOT vegetation NDVI data. *International Journal of Remote Sensing* 26(20):4485–4498. doi:10.1080/01431160500168686
- Wang XQ, Jiang J, Wang YC, Luo WL, Song CW, Chen JJ (2006) Responses of ephemeral plant germination and growth to water and heat conditions in the southern part of Gurbantunggut Desert. *Chinese Science Bulletin* 51:110–116. doi:10.1007/s11434-006-8214-z
- Wang LX, D'Odorico P, Evans JP, Eldridge DJ, McCabe MF, Caylor KK, King EG (2012) Dryland ecohydrology and climate change: critical issues and technical advances. *Hydrology and Earth System Sciences* 16(8):2585–2603. doi:10.5194/hess-16-2585-2012
- Wen LJ, Jin JM (2012) Modelling and analysis of the impact of irrigation on local arid climate over northwest China. *Hydrological Processes* 26(3):445–453. doi:10.1002/Hyp.8142
- White MA, Thornton PE, Running SW (1997) A continental phenology model for monitoring vegetation responses to interannual climatic variability. *Global Biogeochem Cycles* 11(2):217–234. doi:10.1029/97GB00330
- Xia JY, Wan SQ (2012) The effects of warming-shifted plant phenology on ecosystem carbon exchange are regulated by precipitation in a semi-arid grassland. *Plos One* 7(2):e32088. doi:10.1371/journal.pone.0032088
- Yu HY, Luedeling E, Xu JC (2010) Winter and spring warming result in delayed spring phenology on the Tibetan Plateau. *Proc Natl Acad Sci U S A* 107(51):22151–22156. doi:10.1073/pnas.1012490107
- Zhang XY, Friedl MA, Schaaf CB, Strahler AH (2004) Climate controls on vegetation phenological patterns in northern mid- and high latitudes inferred from MODIS data. *Glob Chang Biol* 10(7):1133–1145. doi:10.1111/j.1529-8817.2003.00784.x
- Zhang T, Sun Y, Song YC, Tian CY, Feng G (2011) On-site growth response of a desert ephemeral plant, *Plantago minuta*, to indigenous arbuscular mycorrhizal fungi in a central Asia desert. *Symbiosis* 55(2):77–84. doi:10.1007/s13199-011-0148-9
- Zhang MJ, Wang SJ, Li ZQ, Wang FT (2012a) Glacier area shrinkage in China and its climatic background during the past half century. *Journal of Geographical Sciences* 22(1):15–28. doi:10.1007/s11442-012-0908-3
- Zhang T, Tian CY, Sun Y, Bai DS, Feng G (2012b) Dynamics of arbuscular mycorrhizal fungi associated with desert ephemeral plants in Gurbantunggut Desert. *Journal of Arid Land* 4(1):43–51. doi:10.3724/Sp.J.1227.2012.00042